# Deep Image and Deep Dose Formation in CT

Marc Kachelrieß
German Cancer Research Center (DKFZ)
Heidelberg, Germany
www.dkfz.de/ct

DEUTSCHES KREBSFORSCHUNGSZENTRUM IN DER HELMHOLTZ-GEMEINSCHAFT

## Overview Publications in PubMed

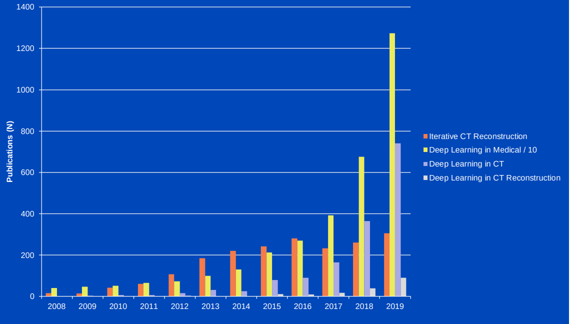


2019 estimated for the whole year based on the values as of July 17, 2019.

## Fully Connected Neural Network

- Each layer fully connects to previous layer
- Difficult to train (many parameters in *W* and *b*)
- Spatial relations not necessarily preserved

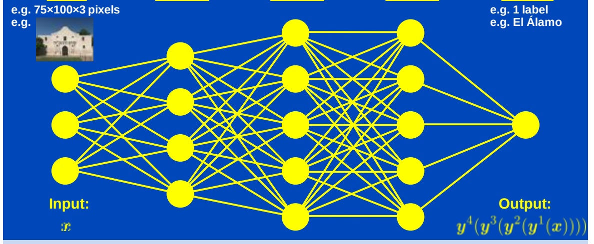


$y(x) = f(W\cdot x+b)$ with $f(x) = (f(x_1), f(x_2), \dots)$ point-wise scalar, e.g. $f(x) = x\vee 0 = \mathrm{ReLU}$

# Convolutional Neural Network (CNN)

- Replace dense *W* in $y(x) = f(W \cdot x + b)$ by a sparse matrix *W* with sparsity being of convolutional type.
- CNNs consist (mainly) of convolutional layers.
- Convolutional layers are not fully connected.
- Convolutional layers are connected by small, say 3×3, convolution kernels whose entries need to be found by training.
- CNNs preserve spatial relations to some extent.

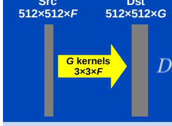


$$D_{i,j,g} = \sum_f S_{i,j,f} * K^g_{i,j,f} = \sum_{a,b,f} S_{i-a,j-b,f} K^g_{a,b,f}$$

Attention: No convolution in depth direction!

# U-Net[1]

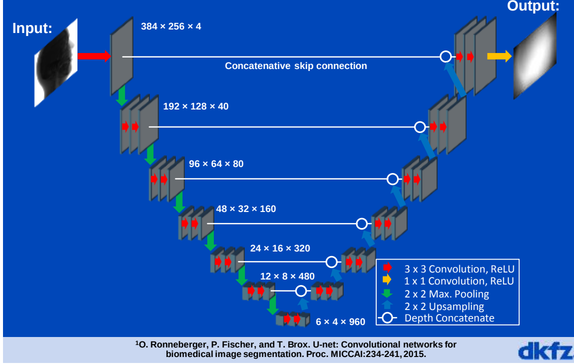


[1]O. Ronneberger, P. Fischer, and T. Brox. U-net: Convolutional networks for biomedical image segmentation. Proc. MICCAI:234-241, 2015.

# Generative Adversarial Network[1] (GAN)

- Useful, if no direct ground truth (GT) is available, the training data are unpaired, unsupervised learning

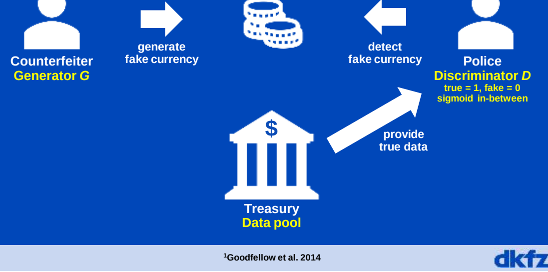


[1]Goodfellow et al. 2014

# Outline

1. Making up data
2. Noise reduction
3. Replacement of lengthy computations
4. Image reconstruction

# Part 1:

# Making up Data

# Limited Angle Example

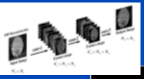

GT FBP (150°) CNN

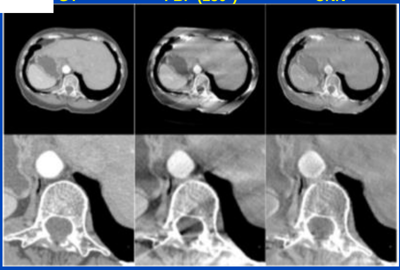

Image Prediction for Limited-Angle Tomography via Deep Learning with Convolutional Neural Network.
Hanming Zhang, Liang Li, Kai Qiao, Linyuan Wang, Bin Yan, Lei Li, Guoen Hu. arXiv 2016.

## MAR Example

- Deep CNN-driven patch-based combination of the advantages of several MAR methods trained on simulated artifacts

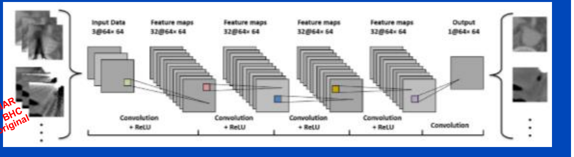


- followed by segmentation into tissue classes
- followed by forward projection of the CNN prior and replacement of metal areas of the original sinogram
- followed by reconstruction

Yanbo Zhang and Hengyong Yu. Convolutional Neural Network Based Metal Artifact Reduction in X-Ray Computed Tomography. TMI 37(6):1370-1381, June 2018.

dkfz.

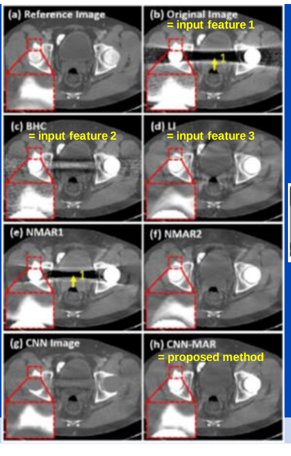



dkfz.

## Sparse View Restoration Example

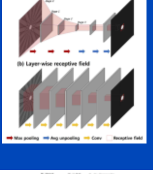

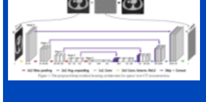

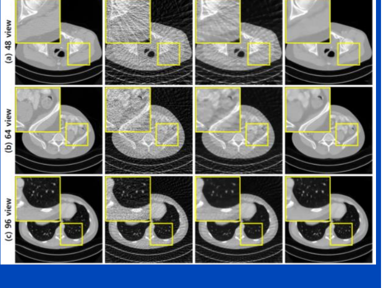


Yo Seob Han, Jaejun Yoo and Jong Chul Ye. Deep Residual Learning for Compressed Sensing CT Reconstruction via Persistent Homology Analysis. ArXiv 2016.

dkfz.

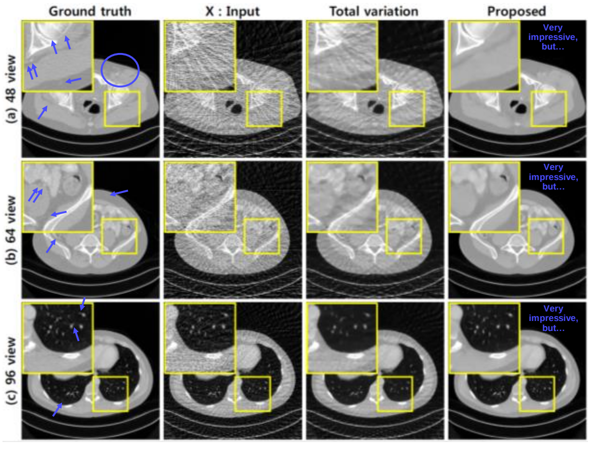


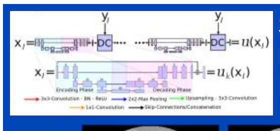


## Sparse CT Recon with Data Consistency Layers (DCLs)

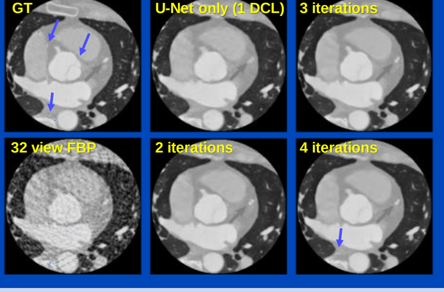


A. Kofler, M. Haltmeier, C. Kolbitsch, M. Kachelrieß, and M. Dewey. A U-Nets Cascade for Sparse View Computed Tomography, MICCAI 2018

dkfz.

## Part 2:

## Noise Reduction

dkfz.

## Noise Removal Example 1

- 3-layer CNN uses low dose and corresponding normal dose image patches for training

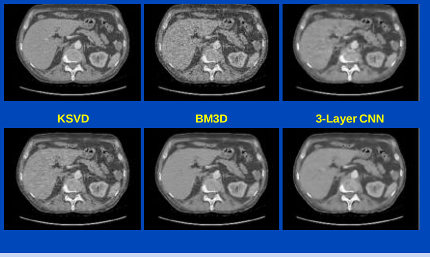


Hu Chen, Yi Zhan, Weihua Zhang, Peixi Liao, Ke Li, Jiliu Zhou, and Ge Wang. Low-dose CT via convolutional neural network. Biomedical Optics Express 8(2):278381, February 2017.

## Noise Removal Example 2

- Task: Reduce noise from low dose CT images.
- A conditional generative adversarial networks (GAN) is used
- Generator *G*:
  - 3D CNN that operates on small cardiac CT sub volumes
  - Seven 3×3×3 convolutional layers yielding a receptive field of 15×15×15 voxels for each destination voxel
  - Depths (features) from 32 to 128
  - Batch norm only in the hidden layers
  - Subtracting skip connection
- Discriminator *D*:
  - Sees either routine dose image or a generator-denoised low dose image
  - Two 3×3×3 layers followed by several 3×3 layers with varying strides
  - Feedback from *D* prevents smoothing.
- Training:
  - Unenhanced (why?) patient data acquired with Philips Briliance iCT 256 at 120 kV.
  - Two scans (why?) per patient, one with 0.2 mSv and one with 0.9 mSv effective dose.

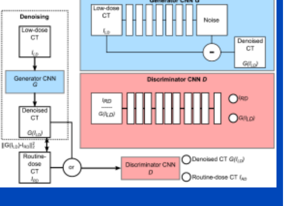


J. Wolterink, T. Leiner, M. Viergever, and I. Išgum. Generative Adversarial Networks for Noise Reduction in Low-Dose CT. IEEE TMI 36(12):2536-2544, Dec. 2017.

## Noise Removal Example 2

- $G_1$ and $G_2$ include supervised learning and thus perform only with phantom measurements.
- $G_3$ is unsupervised.
- $G_3$ is said to generate images with a more similar appearance to the routine-dose CT. Feedback from the discriminator *D* prevents smoothing the image.

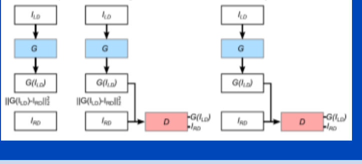


J. Wolterink, T. Leiner, M. Viergever, and I. Išgum. Generative Adversarial Networks for Noise Reduction in Low-Dose CT. IEEE TMI 36(12):2536-2544, Dec. 2017.

# Noise Removal Example 2

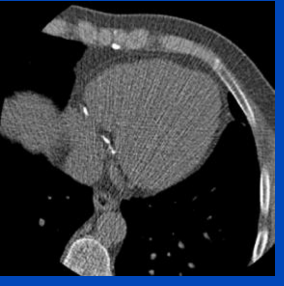

Low dose image (0.2 mSv)

J. Wolterink, T. Leiner, M. Viergever, and I. Išgum. Generative Adversarial Networks for Noise Reduction in Low-Dose CT. IEEE TMI 36(12):2536-2544, Dec. 2017.

dkfz.

# Noise Removal Example 2

iDose level 3 reconstruction (0.2 mSv)

J. Wolterink, T. Leiner, M. Viergever, and I. Išgum. Generative Adversarial Networks for Noise Reduction in Low-Dose CT. IEEE TMI 36(12):2536-2544, Dec. 2017.

dkfz.

# Noise Removal Example 2

Denoised low dose image (0.2 mSv)

J. Wolterink, T. Leiner, M. Viergever, and I. Išgum. Generative Adversarial Networks for Noise Reduction in Low-Dose CT. IEEE TMI 36(12):2536-2544, Dec. 2017.

dkfz.

# Noise Removal Example 2

Normal dose image (0.9 mSv)

J. Wolterink, T. Leiner, M. Viergever, and I. Išgum. Generative Adversarial Networks for Noise Reduction in Low-Dose CT. IEEE TMI 36(12):2536-2544, Dec. 2017.

dkfz.

# Noise Removal Example 3

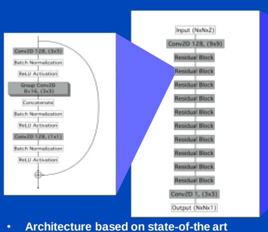


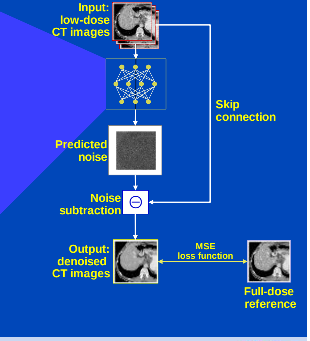


- Architecture based on state-of-the art networks for image classification (ResNet).
- 32 conv layers with skip connections
- About 2 million tunable parameters in total
- Input is arbitrarily-size stack of images, with a fixed number of adjacent slices in the channel/feature dimension.

Andrew D. Missert, Shuai Leng, Lifeng Yu, and Cynthia H. McCollough. Noise Subtraction for Low-Dose CT Images Using a Deep Convolutional Neural Network. Proceedings of the 5th CT-Meeting: 399-402, 2018.

dkfz.

# Noise Removal Example 3

Low dose images (1/4 of full dose)

Andrew D. Missert, Shuai Leng, Lifeng Yu, and Cynthia H. McCollough. Noise Subtraction for Low-Dose CT Images Using a Deep Convolutional Neural Network. Proceedings of the 5th CT-Meeting: 399-402, 2018.

dkfz.

## Noise Removal Example 3

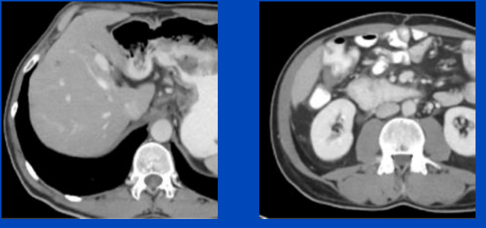

Denoised low dose

Andrew D. Missert, Shuai Leng, Lifeng Yu, and Cynthia H. McCollough. Noise Subtraction for Low-Dose CT Images Using a Deep Convolutional Neural Network. Proceedings of the 5th CT-Meeting: 399-402, 2018.

## Noise Removal Example 3

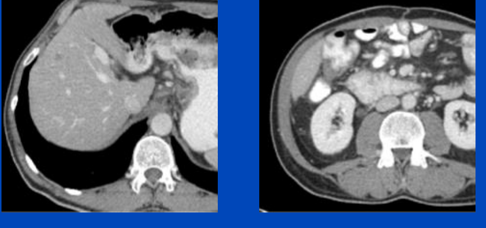

Full dose

Andrew D. Missert, Shuai Leng, Lifeng Yu, and Cynthia H. McCollough. Noise Subtraction for Low-Dose CT Images Using a Deep Convolutional Neural Network. Proceedings of the 5th CT-Meeting: 399-402, 2018.

## Noise Removal Example 3

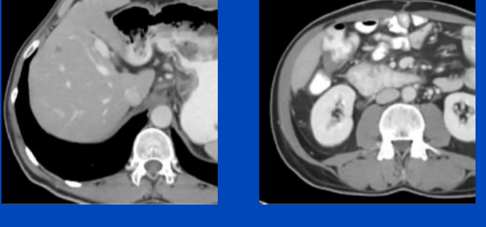

Denoised full dose

Andrew D. Missert, Shuai Leng, Lifeng Yu, and Cynthia H. McCollough. Noise Subtraction for Low-Dose CT Images Using a Deep Convolutional Neural Network. Proceedings of the 5th CT-Meeting: 399-402, 2018.

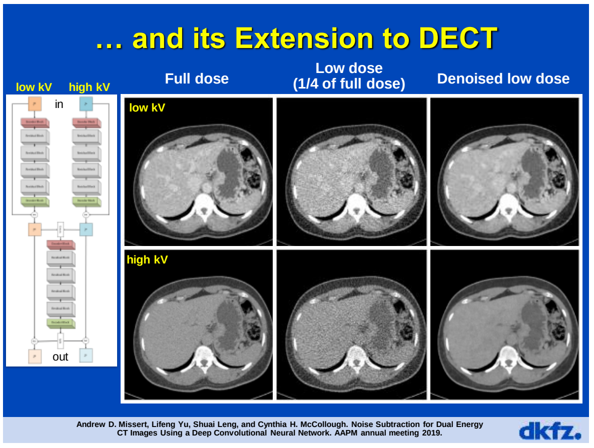
… and its Extension to DECT
low kV
high kV
in
out
Full dose
Low dose
(1/4 of full dose)
Denoised low dose
low kV
high kV
Andrew D. Missert, Lifeng Yu, Shuai Leng, and Cynthia H. McCollough. Noise Subtraction for Dual Energy CT Images Using a Deep Convolutional Neural Network. AAPM annual meeting 2019.
dkfz.

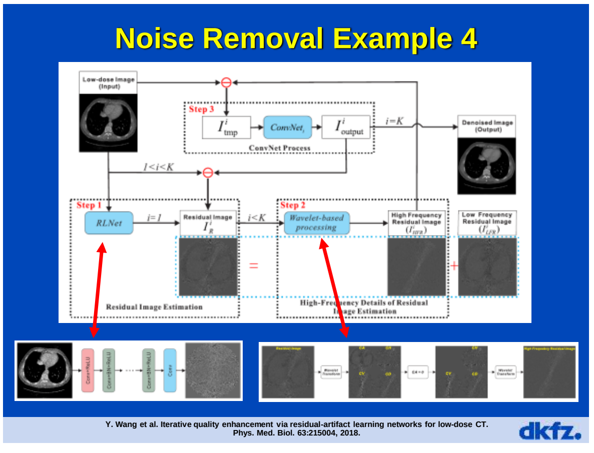
Noise Removal Example 4
Low-dose Image (Input)
Step 3
ConvNet Process
i=K
Denoised Image (Output)
1<i<K
Step 1
RLNet
i=1
Residual Image
i<K
Step 2
Wavelet-based processing
High Frequency Residual Image
Low Frequency Residual Image
Residual Image Estimation
High-Frequency Details of Residual Image Estimation
Y. Wang et al. Iterative quality enhancement via residual-artifact learning networks for low-dose CT. Phys. Med. Biol. 63:215004, 2018.
dkfz.

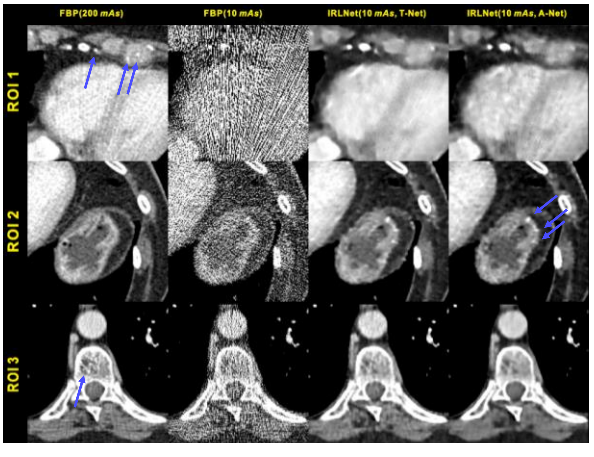
FBP(200 mAs)
FBP(10 mAs)
IRLNet(10 mAs, T-Net)
IRLNet(10 mAs, A-Net)
ROI 1
ROI 2
ROI 3

# Noise Removal Example 5

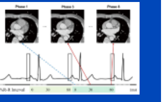

- ECG-based TCM yields cardiac phases with high noise.
- Train a cycle GAN that learns from the low noise phases to remove noise in the high noise phases.
- 50 patient cases used for training.
- Nice results!

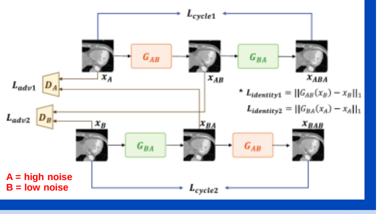


E. Kang, J.C. Ye et al. Cycle-consistent adversarial denoising network for multiphase coronary CT angiography. Med. Phys. 46(2), February 2019.

dkfz.

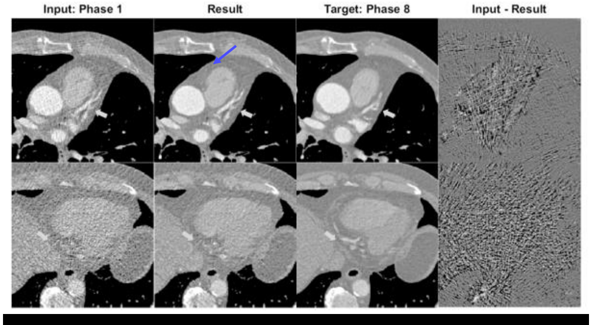


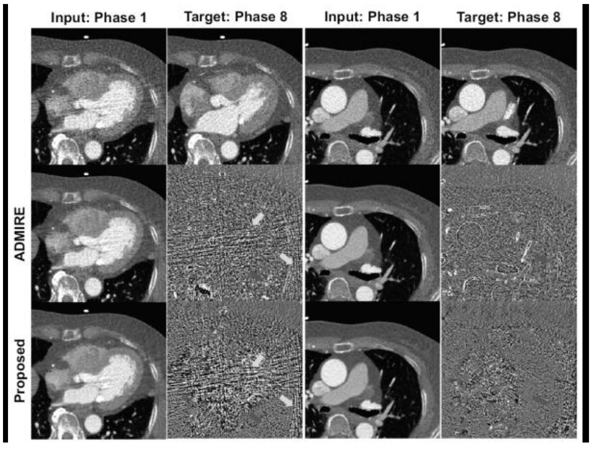

## Noise Removal Example 6
## Canon‘s AiCE

- Ba… CNN
- Tr…
  pr…
- FI… a
  hi…

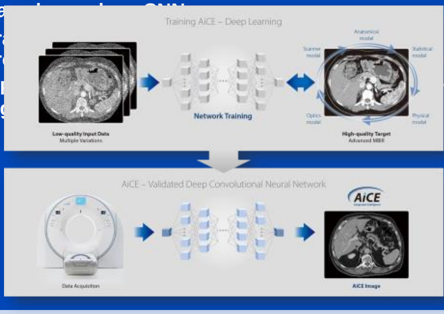


Information taken from https://global.medical.canon/products/computed-tomography/aice_dlr

dkfz.

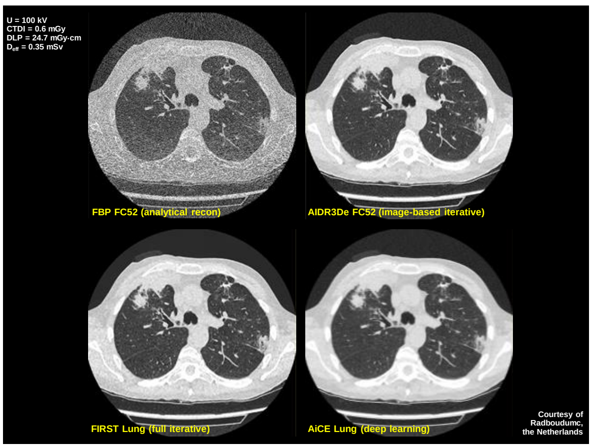


## Noise Removal Example 7
## GE‘s True Fidelity

- Based on a deep CNN
- Trained to restore low-dose CT data to match the properties of Veo, the model-based IR of GE.
- No information can be obtained in how the training is conducted for the product implementation.

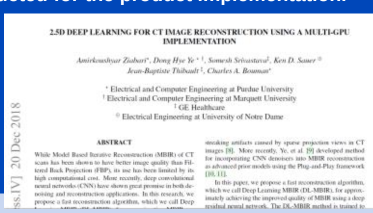

**2.5D DEEP LEARNING FOR CT IMAGE RECONSTRUCTION USING A MULTI-GPU IMPLEMENTATION**

*Amirkoushyar Ziabari*, Dong Hye Ye * †, Somesh Srivastava‡, Ken D. Sauer ◎ Jean-Baptiste Thibault ‡, Charles A. Bouman**

* Electrical and Computer Engineering at Purdue University
† Electrical and Computer Engineering at Marquett University
‡ GE Healthcare
◎ Electrical Engineering at University of Notre Dame

ss.IV] 20 Dec 2018

**ABSTRACT**

While Model Based Iterative Reconstruction (MBIR) of CT scans has been shown to have better image quality than Filtered Back Projection (FBP), its use has been limited by its high computational cost. More recently, deep convolutional neural networks (CNN) have shown great promise in both denoising and reconstruction applications. In this research, we propose a fast reconstruction algorithm, which we call Deep

streaking artifacts caused by sparse projection views in CT images [8]. More recently, Ye, et al. [9] developed method for incorporating CNN denoisers into MBIR reconstruction as advanced prior models using the Plug-and-Play framework [10, 11].

In this paper, we propose a fast reconstruction algorithm, which we call Deep Learning MBIR (DL-MBIR), for approximately achieving the improved quality of MBIR using a deep residual neural network. The DL-MBIR method is trained to

dkfz.

## No Low Noise Images Required to Train Denoising Networks!

**Noise2Noise: Learning Image Restoration without Clean Data**

Jaakko Lehtinen[1 2] Jacob Munkberg[1] Jon Hasselgren[1] Samuli Laine[1] Tero Karras[1] Miika Aittala[3] Timo Aila[1]

**Abstract**

We apply basic statistical reasoning to signal reconstruction by machine learning – learning to map corrupted observations to clean signals – with a simple and powerful conclusion: it i… ble to learn to restore images by only lo… corrupted examples, at performance at an… times exceeding training using clean data, … explicit image priors or likelihood mode… corruption. In practice, we show that … model learns photographic noise removal … ing synthetic Monte Carlo images, and re… tion of undersampled MRI scans – all co… by different processes – based on noisy d…

renderings of a synthetic scene, etc. Significant advances have been reported in several applications, including Gaussian denoising, de-JPEG, text removal (Mao et al., 2016), super-resolution (Ledig et al., 2017), colorization (Zhang et al., 2016), and image inpainting (Iizuka et al., 2017). Yet,

CV] 9 Aug 2018


J. Lehtinen et al. Noise2Noise: Learning Image Restoration without Clean Data. https://arxiv.org/pdf/1803.04189.pdf. August 2018.

dkfz.

## No Low Noise Images Required to Train Denoising Networks!

- Estimation can be regarded as ML estimation by interpreting the loss function as the negative log likelihood.
- On expectation, the estimate remains unchanged if we replace the targets with random numbers whose expectations match the targets.
- Input-conditioned target distributions $p(y|x)$ can be replaced with arbitrary distributions that have the same conditional expected values.
- Consequently, we may corrupt the training targets of a neural network with zero-mean noise without changing what the network learns.
- Useful for image restoration tasks where the expectation of the corrupted input data is the clean target that we seek to restore.
- Denoising possible if at least two realizations of each image are available.

J. Lehtinen et al. Noise2Noise: Learning Image Restoration without Clean Data. https://arxiv.org/pdf/1803.04189.pdf. August 2018.

dkfz.

## Noise Removal Example 8 (Training on Noisy CT Targets)

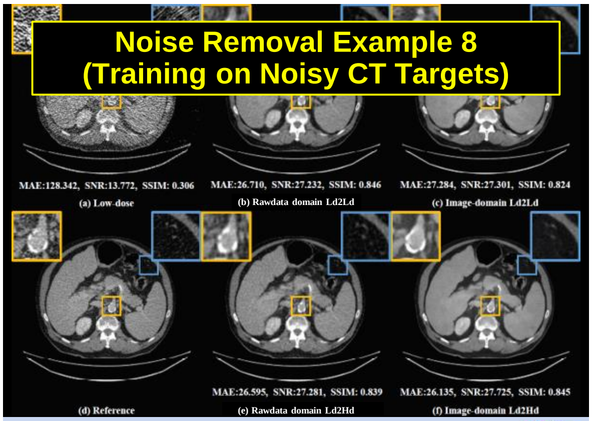


N. Yuan, J. Zhou, J. Qi. Low-dose CT image denoising without high-dose reference images. Proc. 15th Fully3D Meeting 110721C:1-5, 2019.

dkfz.

# Part 3:

# Replacement of Lengthy Computations Fast Physics

## Empirical Shading Correction: ScatterNet

- Net to convert CBCT log (why?) rawdata into artifact-free data.
- Net architecture:
  - Small receptive field spectrum converter block adapts the attenuation values.
  - Residual U-Net then follows to account for scatter.
- Pixel-wise loss function comparing the corrected CBCT projections with those of the reference shading correction method.
- Reference shading correction method:
  - Use data from a clinical CT scan as an artifact-free prior.
  - Intensity domain frequency split between planning CT and CBCT:
    - » Deformably register planning CT onto CBCT and forward project and exponentiate to obtain "ideal" intensity data
    - » Scale CBCT intensities to match the prior CT intensities
    - » Corrected intensities = LP(forward proj. CT)+HP(scaled uncorr. CBCT)
- ScatterNet replaces the previous correction method and thus speeds up computation and does not make use of the planning CT.

D. Hansen, K. Parodi et al. ScatterNet: A convolutional neural network for cone-beam CT intensity correction, Med. Phys., Sep. 2018.

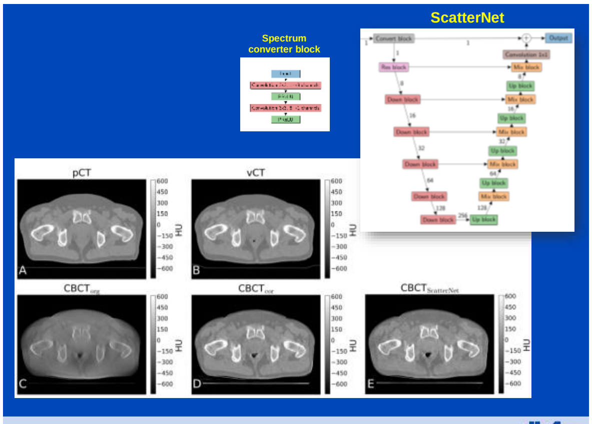


D. Hansen, K. Parodi et al. ScatterNet: A convolutional neural network for cone-beam CT intensity correction, Med. Phys., Sep. 2018.

# Deep Scatter Estimation

# Scatter Correction

## Scatter suppression

- Anti-scatter grids
- Collimators
- …

## Scatter estimation

- Monte Carlo simulation
- Kernel-based approaches
- Boltzmann transport
- Primary modulation
- Beam blockers
- …

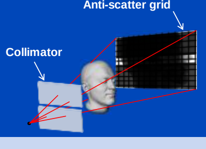


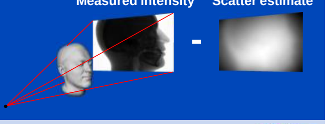


# Monte Carlo Scatter Estimation

- Simulation of photon trajectories according to physical interaction probabilities.
- Simulating a large numb… …ries well approximat…

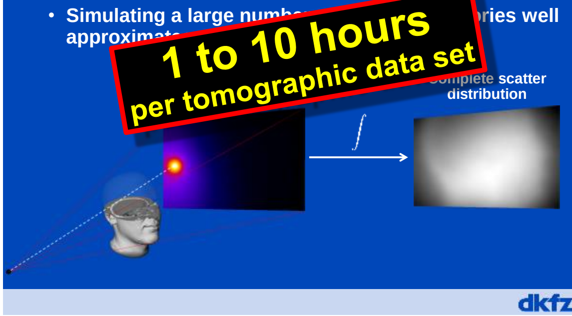

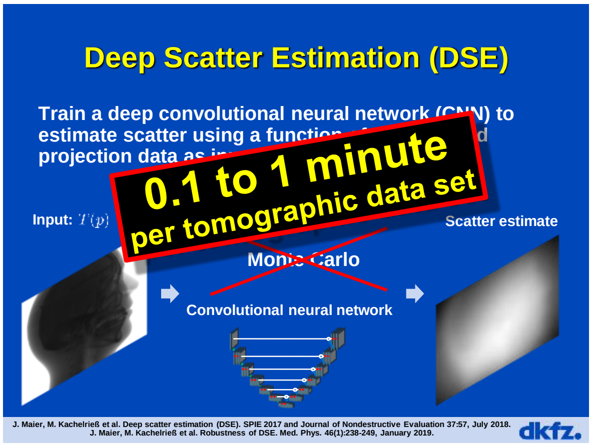
Deep Scatter Estimation (DSE)
Train a deep convolutional neural network (CNN) to
estimate scatter using a function
projection data as
0.1 to 1 minute
per tomographic data set
Input: $T(p)$
Scatter estimate
Monte Carlo
Convolutional neural network
J. Maier, M. Kachelrieß et al. Deep scatter estimation (DSE). SPIE 2017 and Journal of Nondestructive Evaluation 37:57, July 2018.
J. Maier, M. Kachelrieß et al. Robustness of DSE. Med. Phys. 46(1):238-249, January 2019.
dkfz.

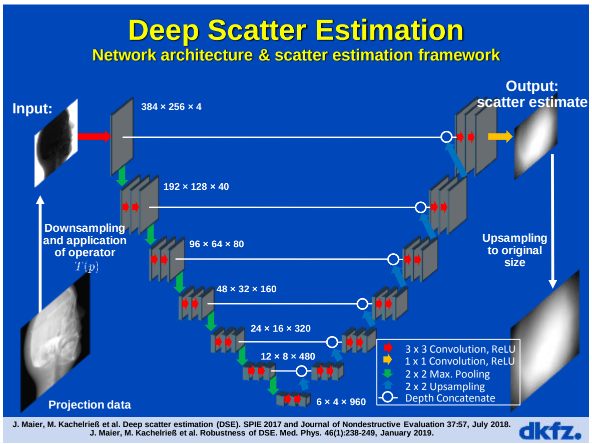
Deep Scatter Estimation
Network architecture & scatter estimation framework
Input:
Output:
scatter estimate
384 × 256 × 4
192 × 128 × 40
96 × 64 × 80
48 × 32 × 160
24 × 16 × 320
12 × 8 × 480
6 × 4 × 960
Downsampling
and application
of operator
$T(p)$
Upsampling
to original
size
Projection data
3 x 3 Convolution, ReLU
1 x 1 Convolution, ReLU
2 x 2 Max. Pooling
2 x 2 Upsampling
Depth Concatenate
J. Maier, M. Kachelrieß et al. Deep scatter estimation (DSE). SPIE 2017 and Journal of Nondestructive Evaluation 37:57, July 2018.
J. Maier, M. Kachelrieß et al. Robustness of DSE. Med. Phys. 46(1):238-249, January 2019.
dkfz.

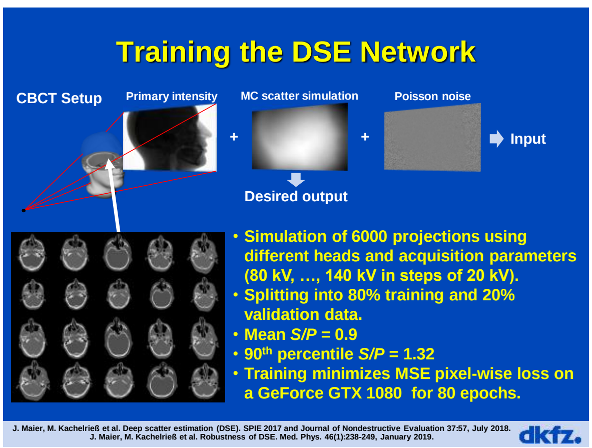
Training the DSE Network
CBCT Setup
Primary intensity
MC scatter simulation
Poisson noise
+
+
Input
Desired output
• Simulation of 6000 projections using different heads and acquisition parameters (80 kV, …, 140 kV in steps of 20 kV).
• Splitting into 80% training and 20% validation data.
• Mean $S/P$ = 0.9
• 90th percentile $S/P$ = 1.32
• Training minimizes MSE pixel-wise loss on a GeForce GTX 1080 for 80 epochs.
J. Maier, M. Kachelrieß et al. Deep scatter estimation (DSE). SPIE 2017 and Journal of Nondestructive Evaluation 37:57, July 2018.
J. Maier, M. Kachelrieß et al. Robustness of DSE. Med. Phys. 46(1):238-249, January 2019.
dkfz.

# Testing of the DSE Network for Simulated Data (at 120 kV)

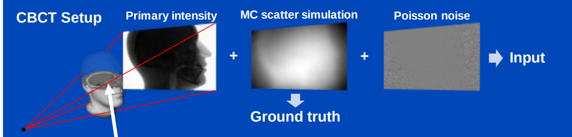


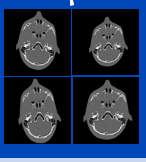

- Application of the DSE network to predict scatter for simulated data of a head (different from training data).

J. Maier, M. Kachelrieß et al. Deep scatter estimation (DSE). SPIE 2017 and Journal of Nondestructive Evaluation 37:57, July 2018.
J. Maier, M. Kachelrieß et al. Robustness of DSE. Med. Phys. 46(1):238-249, January 2019.

dkfz.

# PEP

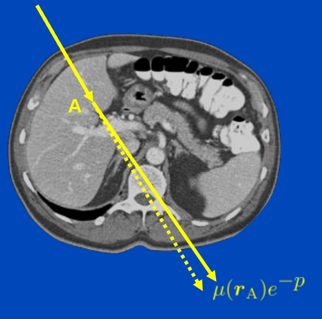


dkfz.

# PEP

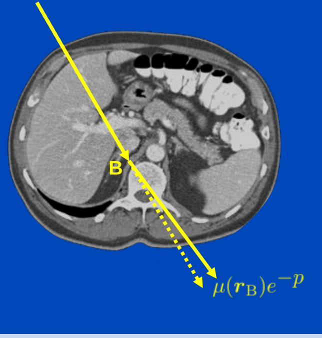


dkfz.

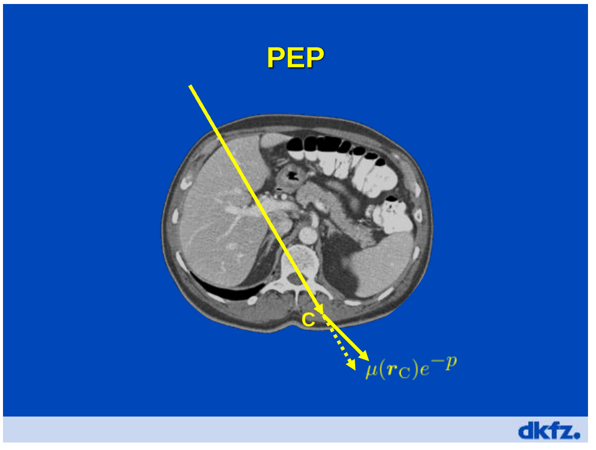
PEP
C
$\mu(\boldsymbol{r}_\mathrm{C})e^{-p}$
dkfz.

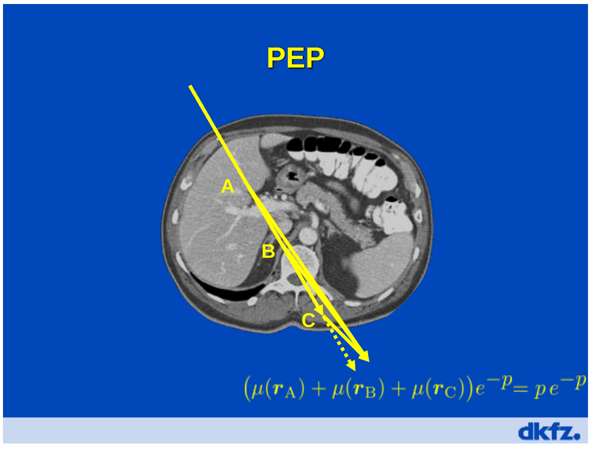
PEP
A
B
C
$(\mu(\boldsymbol{r}_\mathrm{A})+\mu(\boldsymbol{r}_\mathrm{B})+\mu(\boldsymbol{r}_\mathrm{C}))e^{-p} = p\,e^{-p}$
dkfz.

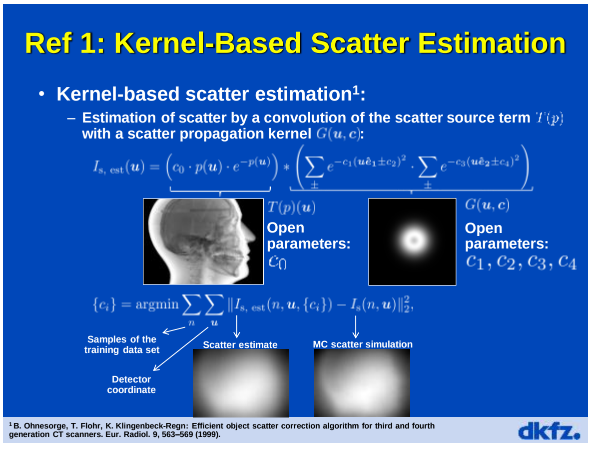
Ref 1: Kernel-Based Scatter Estimation
• Kernel-based scatter estimation[1]:
– Estimation of scatter by a convolution of the scatter source term $T(p)$ with a scatter propagation kernel $G(u, c)$:
$I_{\mathrm{s,\,est}}(\boldsymbol{u}) = \underbrace{\left(c_0 \cdot p(\boldsymbol{u}) \cdot e^{-p(\boldsymbol{u})}\right)}_{T(p)(\boldsymbol{u})} * \underbrace{\left(\sum_{\pm} e^{-c_1(\boldsymbol{u}\hat{\boldsymbol{e}}_1 \pm c_2)^2} \cdot \sum_{\pm} e^{-c_3(\boldsymbol{u}\hat{\boldsymbol{e}}_2 \pm c_4)^2}\right)}_{G(\boldsymbol{u},\boldsymbol{c})}$
Open parameters: $c_0$
Open parameters: $c_1, c_2, c_3, c_4$
$\{c_i\} = \operatorname{argmin} \sum_n \sum_{\boldsymbol{u}} \| I_{\mathrm{s,\,est}}(n, \boldsymbol{u}, \{c_i\}) - I_\mathrm{s}(n, \boldsymbol{u}) \|_2^2,$
Samples of the training data set
Detector coordinate
Scatter estimate
MC scatter simulation
[1] B. Ohnesorge, T. Flohr, K. Klingenbeck-Regn: Efficient object scatter correction algorithm for third and fourth generation CT scanners. Eur. Radiol. 9, 563–569 (1999).
dkfz.

## Ref 2: Hybrid Scatter Estimation

- **Hybrid scatter estimation**[2] **:**
  - **Estimation of scatter by a convolution of the scatter source term $T(p)$ with a scatter propagation kernel $G(u, c)$:**

$$I_{\mathrm{s,\,est}}(\boldsymbol{u}) = \underbrace{\left(c_0 \cdot p(\boldsymbol{u}) \cdot e^{-p(\boldsymbol{u})}\right)}_{T(p)(\boldsymbol{u})} * \underbrace{\left(\sum_{\pm} e^{-c_1(\boldsymbol{u}\hat{\boldsymbol{e}}_1 \pm c_2)^2} \cdot \sum_{\pm} e^{-c_3(\boldsymbol{u}\hat{\boldsymbol{e}}_2 \pm c_4)^2}\right)}_{G(\boldsymbol{u}, \boldsymbol{c})}$$

$T(p)(\boldsymbol{u})$

**Open parameters:** $c_0$

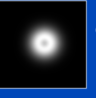

$G(\boldsymbol{u}, \boldsymbol{c})$

**Open parameters:** $c_1, c_2, c_3, c_4$

$$\{c_i\}_n = \operatorname{argmin} \sum_{\boldsymbol{u}} \| I_{\mathrm{s,\,est}}(n, \boldsymbol{u}, \{c_i\}) - I_{\mathrm{s}}(n, \boldsymbol{u}) \|_2^2,$$

**Samples of the test data set**

**Detector coordinate**

**Scatter estimate**

**Coarse MC simulation**

[2] M. Baer, M. Kachelrieß: Hybrid scatter correction for CT imaging. Phys. Med. Biol. 57, 6849–6867 (2012).

dkfz.

## Results on Simulated Projection Data

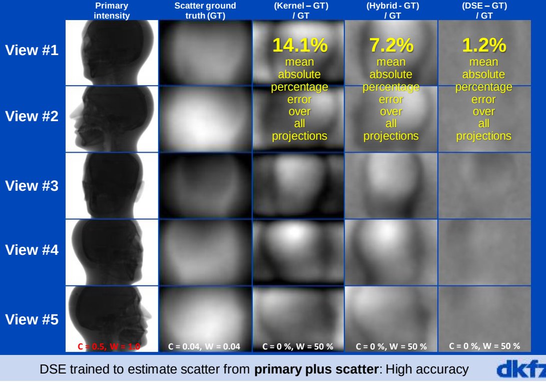


DSE trained to estimate scatter from **primary plus scatter**: High accuracy

dkfz.

## Results on Simulated Projection Data

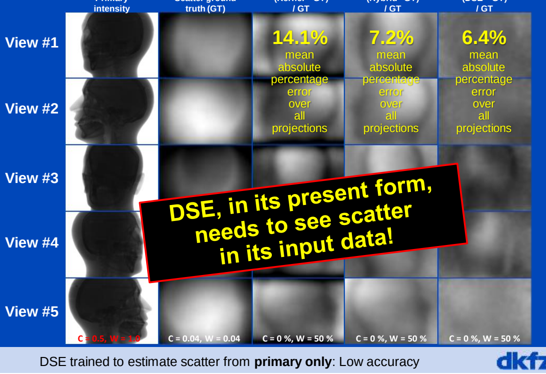


DSE trained to estimate scatter from **primary only**: Low accuracy

dkfz.

# Results on Simulated Projection Data

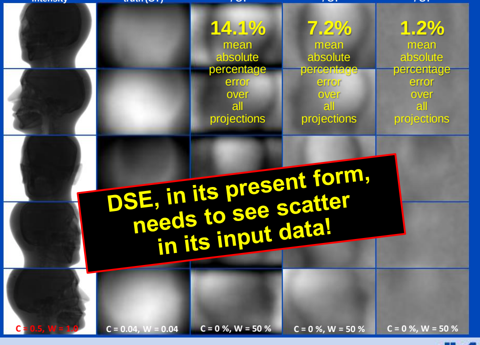


DSE trained to estimate scatter from **primary plus scatter**: High accuracy

# Reconstructions of Simulated Data

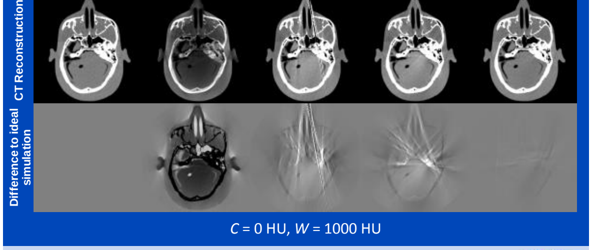


*C* = 0 HU, *W* = 1000 HU

J. Maier, M. Kachelrieß et al. Deep scatter estimation (DSE). SPIE 2017 and Journal of Nondestructive Evaluation 37:57, July 2018.
J. Maier, M. Kachelrieß et al. Robustness of DSE. Med. Phys. 46(1):238-249, January 2019.

# Testing of the DSE Network for Measured Data (120 kV)

DKFZ table-top CT

- Measurement of a head phantom at our in-house table-top CT.
- Slit scan measurement serves as ground truth.

Measurement to be corrected

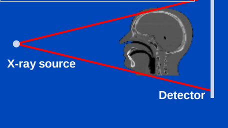


Ground truth: slit scan

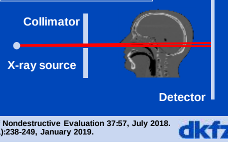


J. Maier, M. Kachelrieß et al. Deep scatter estimation (DSE). SPIE 2017 and Journal of Nondestructive Evaluation 37:57, July 2018.
J. Maier, M. Kachelrieß et al. Robustness of DSE. Med. Phys. 46(1):238-249, January 2019.

## Reconstructions of Measured Data

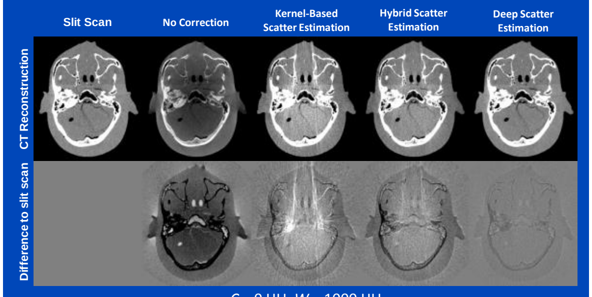


$C$ = 0 HU, $W$ = 1000 HU

J. Maier, M. Kachelrieß et al. Deep scatter estimation (DSE). SPIE 2017 and Journal of Nondestructive Evaluation 37:57, July 2018.
J. Maier, M. Kachelrieß et al. Robustness of DSE. Med. Phys. 46(1):238-249, January 2019.

A simple detruncation was applied to the rawdata before reconstruction. Images were clipped to the FOM before display. $C$ = -200 HU, $W$ = 1000 HU.

## Truncated DSE[1,2]

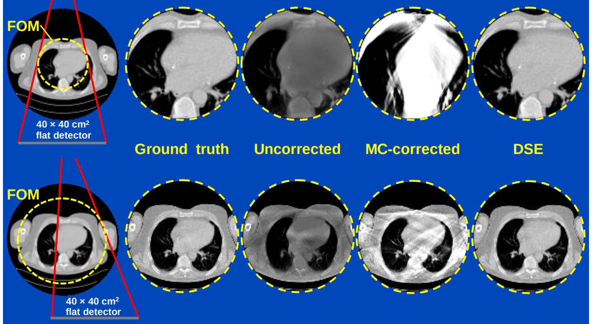


To learn why MC fails at truncated data and what significant efforts are necessary to cope with that situation see [Kachelrieß et al. Effect of detruncation on the accuracy of MC-based scatter estimation in truncated CBCT. Med. Phys. 45(8):3574-3590, August 2018].

[1]J. Maier, M. Kachelrieß et al. Deep scatter estimation (DSE) for truncated cone-beam CT (CBCT). RSNA 2018.
[2]J. Maier, M. Kachelrieß et al. Robustness of DSE. Med. Phys. 46(1):238-249, January 2019.

## Generalization to Different Anatomical Regions

| DSE | Head | Thorax | Abdomen |
|---|---|---|---|
| Head | 1.2 | 21.1 | 32.7 |
| Thorax | 8.8 | 1.5 | 9.1 |
| Abdomen | 11.9 | 10.9 | 1.3 |
| All data | 1.8 | 1.4 | 1.4 |

Values shown are the mean absolute percentage errors (MAPEs) of the testing data.
Note that thorax and head suffer from truncation due to the small size of the 40×30 cm flat detector.

J. Maier, M. Kachelrieß et al. Deep scatter estimation (DSE). SPIE 2017 and Journal of Nondestructive Evaluation 37:57, July 2018.
J. Maier, M. Kachelrieß et al. Robustness of DSE. Med. Phys. 46(1):238-249, January 2019.

## Conclusions on DSE

- DSE needs about 20 ms per projection. It is a fast and accurate alternative to Monte Carlo (MC) simulations.
- DSE outperforms kernel-based approaches in terms of accuracy and speed.
- Interesting observations
  - DSE can estimate scatter from a single (!) x-ray image.
  - DSE can accurately estimate scatter from a primary+scatter image.
  - DSE cannot accurately estimate scatter from a primary only image.
  - DSE may thus outperform MC even though DSE is trained with MC.
- DSE is not restricted to reproducing MC scatter estimates.
- DSE can rather be trained with any other scatter estimate, including those based on measurements.

dkfz.

## Estimation of Dose Distributions

- Useful to study dose reduction techniques
  - Tube current modulation
  - Prefiltration and shaped filtration
  - Tube voltage settings
  - …
- Useful to estimate patient dose
  - Risk assessment requires segmentation of the organs (difficult)
  - Often semiantropomorphic patient models take over
  - The infamous k-factors that convert DLP into $D_{eff}$ are derived this way, e.g. $k_{chest}$ = 0.014 mSv/mGy/cm
  - …
- Useful for patient-specific CT scan protocol optimization
- However: Dose estimation does not work in real time!

J. Maier, E. Eulig, S. Sawall, and M. Kachelrieß. Real-time patient-specific CT dose estimation using a deep convolutional neural network, Proc. IEEE MIC 2018 and ECR Book of Abstracts 2019. *Best Paper within Machine Learning at ECR 2019!*

dkfz.

## Influence of Bowtie Filter

- Commercial CT-scanners are usually equipped with a bowtie filter in order to optimize the patient dose distribution.
- Monte-Carlo dose calculations or statistical reconstruction algorithms require exact knowledge of the bowtie filter.
- The shape as well as the composition of the bowtie filter is usually not disclosed by the CT vendors.

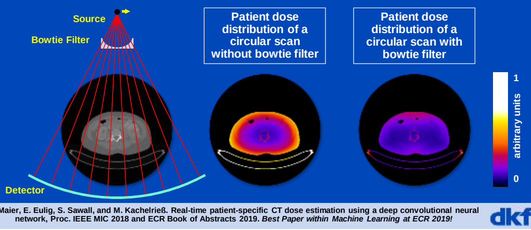


J. Maier, E. Eulig, S. Sawall, and M. Kachelrieß. Real-time patient-specific CT dose estimation using a deep convolutional neural network, Proc. IEEE MIC 2018 and ECR Book of Abstracts 2019. *Best Paper within Machine Learning at ECR 2019!*

dkfz.

## Patient-Specific Dose Estimation

- **Accurate solutions:**
  - Monte Carlo (MC) simulation[1], gold standard, stochastic LBTE solver
  - Analytic linear Boltzmann transport equation (LBTE) solver[2]

  → **Accurate but computationally expensive**
- **Fast alternatives:**
  - Application of patient-specific conversion factors to the DLP[3].
  - Application of look-up tables using MC simulations of phantoms[4].
  - Analytic approximation of CT dose deposition[5].

  → **Fast but less accurate**

[1] G. Jarry et al., "A Monte Carlo-based method to estimate radiation dose from spiral CT", Phys. Med. Biol. 48, 2003.
[2] A. Wang et al., "A fast, linear Boltzmann transport equation solver for computed tomography dose calculation (Acuros CTD)". Med. Phys. 46(2), 2019.
[3] B. Moore et al., "Size-specific dose estimate (SSDE) provides a simple method to calculate organ dose for pediatric CT examinations", Med. Phys. 41, 2014.
[4] A. Ding et al., "VirtualDose: a software for reporting organ doses from CT for adult and pediatric patients", Phys. Med. Biol. 60, 2015.
[5] B. De Man, "Dose reconstruction for real-time patient-specific dose estimation in CT", Med. Phys. 42, 2015.

## Deep Dose Estimation (DDE)

- Combine fast and accurate CT dose estimation using a deep convolutional neural network.
- Train the network to reproduce MC dose estimates given the CT image and a first-order dose estimate.

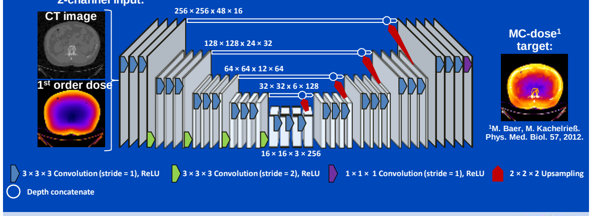


J. Maier, E. Eulig, S. Sawall, and M. Kachelrieß. Real-time patient-specific CT dose estimation using a deep convolutional neural network, Proc. IEEE MIC 2018 and ECR Book of Abstracts 2019. *Best Paper within Machine Learning at ECR 2019!*

## Training and Validation

- Simulation of 1440 circular dual-source CT scans (64×0.6 mm, $FOM_A$ = 50 cm, $FOM_B$ = 32 cm) of thorax, abdomen, and pelvis using 12 different patients.
- Simulation with and without bowtie.
- No data augmentation
- Reconstruction on a 512×512×96 grid with 1 mm voxel size, followed by 2×2×2 binning for dose estimation.
- 9 patients were used for training and 3 for testing.
- DDE was trained for 300 epochs on an Nvidia Quadro P6000 GPU using a mean absolute error pixel-wise loss, the Adam optimizer, and a batch size of 4.
- The same weights and biases were used for all cases.

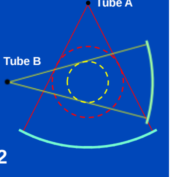


1440 = 12 patients × 20 z-positions × 6 modes (A, A+bowtie, A+bowtie+TCM, B, B+Bowtie, B+bowtie+TCM)

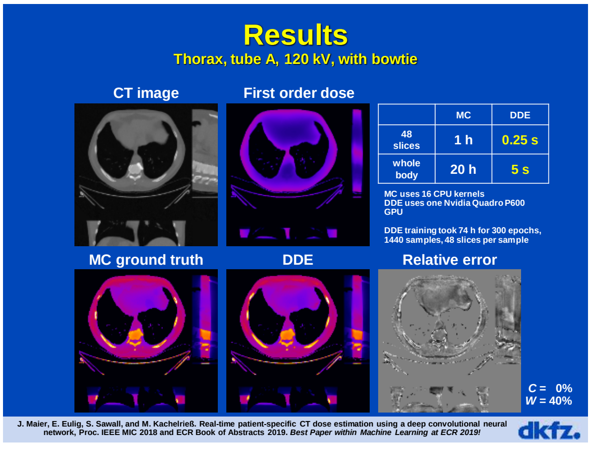
Results
Thorax, tube A, 120 kV, with bowtie
CT image
First order dose
MC
DDE
48 slices
1 h
0.25 s
whole body
20 h
5 s
MC uses 16 CPU kernels
DDE uses one Nvidia Quadro P600 GPU
DDE training took 74 h for 300 epochs, 1440 samples, 48 slices per sample
MC ground truth
DDE
Relative error
C = 0%
W = 40%
J. Maier, E. Eulig, S. Sawall, and M. Kachelrieß. Real-time patient-specific CT dose estimation using a deep convolutional neural network, Proc. IEEE MIC 2018 and ECR Book of Abstracts 2019. Best Paper within Machine Learning at ECR 2019!
dkfz.

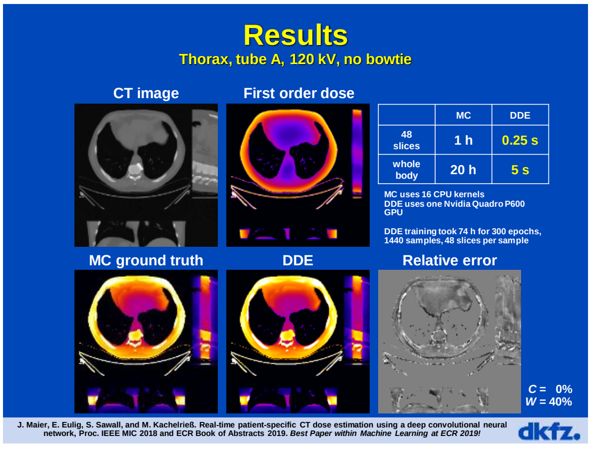
Results
Thorax, tube A, 120 kV, no bowtie
CT image
First order dose
MC
DDE
48 slices
1 h
0.25 s
whole body
20 h
5 s
MC uses 16 CPU kernels
DDE uses one Nvidia Quadro P600 GPU
DDE training took 74 h for 300 epochs, 1440 samples, 48 slices per sample
MC ground truth
DDE
Relative error
C = 0%
W = 40%
J. Maier, E. Eulig, S. Sawall, and M. Kachelrieß. Real-time patient-specific CT dose estimation using a deep convolutional neural network, Proc. IEEE MIC 2018 and ECR Book of Abstracts 2019. Best Paper within Machine Learning at ECR 2019!
dkfz.

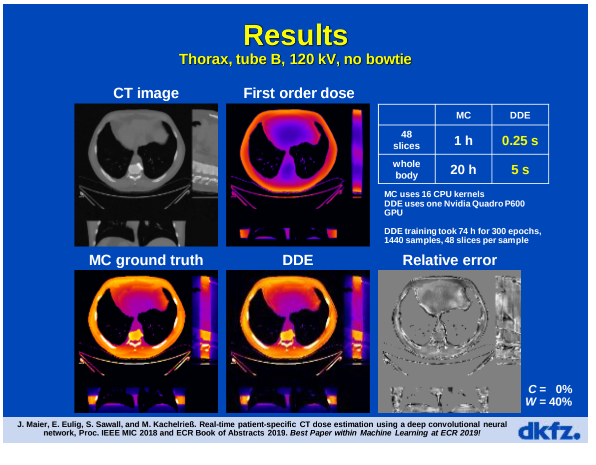
Results
Thorax, tube B, 120 kV, no bowtie
CT image
First order dose
MC
DDE
48 slices
1 h
0.25 s
whole body
20 h
5 s
MC uses 16 CPU kernels
DDE uses one Nvidia Quadro P600 GPU
DDE training took 74 h for 300 epochs, 1440 samples, 48 slices per sample
MC ground truth
DDE
Relative error
C = 0%
W = 40%
J. Maier, E. Eulig, S. Sawall, and M. Kachelrieß. Real-time patient-specific CT dose estimation using a deep convolutional neural network, Proc. IEEE MIC 2018 and ECR Book of Abstracts 2019. Best Paper within Machine Learning at ECR 2019!
dkfz.

## Results
### Abdomen, tube A, 120 kV, with bowtie

CT image · First order dose

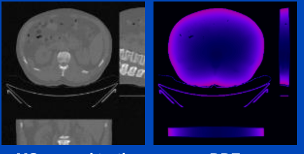

| | MC | DDE |
|---|---|---|
| 48 slices | 1 h | 0.25 s |
| whole body | 20 h | 5 s |

MC uses 16 CPU kernels
DDE uses one Nvidia Quadro P600 GPU

DDE training took 74 h for 300 epochs, 1440 samples, 48 slices per sample

MC ground truth · DDE · Relative error

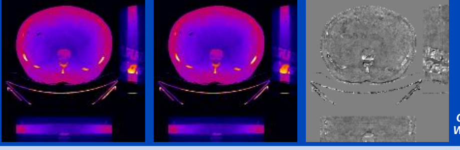

*C* = 0%
*W* = 40%

J. Maier, E. Eulig, S. Sawall, and M. Kachelrieß. Real-time patient-specific CT dose estimation using a deep convolutional neural network, Proc. IEEE MIC 2018 and ECR Book of Abstracts 2019. *Best Paper within Machine Learning at ECR 2019!*

dkfz.

## Results
### Abdomen, tube A, 120 kV, no bowtie

CT image · First order dose

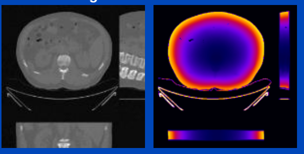

| | MC | DDE |
|---|---|---|
| 48 slices | 1 h | 0.25 s |
| whole body | 20 h | 5 s |

MC uses 16 CPU kernels
DDE uses one Nvidia Quadro P600 GPU

DDE training took 74 h for 300 epochs, 1440 samples, 48 slices per sample

MC ground truth · DDE · Relative error

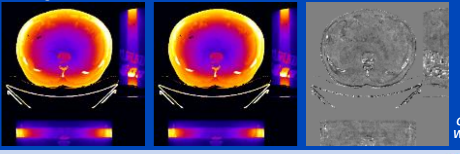

*C* = 0%
*W* = 40%

J. Maier, E. Eulig, S. Sawall, and M. Kachelrieß. Real-time patient-specific CT dose estimation using a deep convolutional neural network, Proc. IEEE MIC 2018 and ECR Book of Abstracts 2019. *Best Paper within Machine Learning at ECR 2019!*

dkfz.

## Results
### Abdomen, tube B, 120 kV, no bowtie

CT image · First order dose

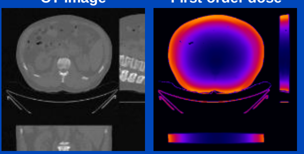

| | MC | DDE |
|---|---|---|
| 48 slices | 1 h | 0.25 s |
| whole body | 20 h | 5 s |

MC uses 16 CPU kernels
DDE uses one Nvidia Quadro P600 GPU

DDE training took 74 h for 300 epochs, 1440 samples, 48 slices per sample

MC ground truth · DDE · Relative error

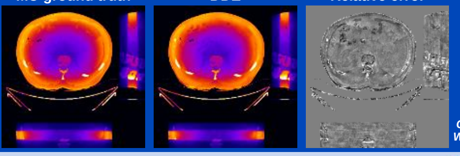

*C* = 0%
*W* = 40%

J. Maier, E. Eulig, S. Sawall, and M. Kachelrieß. Real-time patient-specific CT dose estimation using a deep convolutional neural network, Proc. IEEE MIC 2018 and ECR Book of Abstracts 2019. *Best Paper within Machine Learning at ECR 2019!*

dkfz.

# Results

## Pelvis, tube A, 120 kV, with bowtie

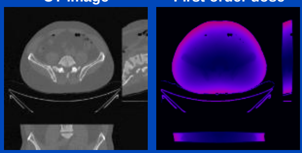


| | MC | DDE |
|---|---|---|
| 48 slices | 1 h | 0.25 s |
| whole body | 20 h | 5 s |

MC uses 16 CPU kernels
DDE uses one Nvidia Quadro P600 GPU

DDE training took 74 h for 300 epochs, 1440 samples, 48 slices per sample

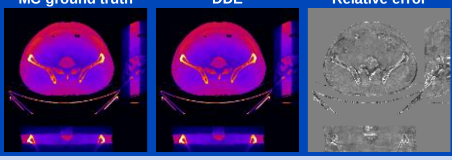


*C* = 0%
*W* = 40%

J. Maier, E. Eulig, S. Sawall, and M. Kachelrieß. Real-time patient-specific CT dose estimation using a deep convolutional neural network, Proc. IEEE MIC 2018 and ECR Book of Abstracts 2019. *Best Paper within Machine Learning at ECR 2019!*

dkfz.

# Results

## Pelvis, tube A, 120 kV, no bowtie

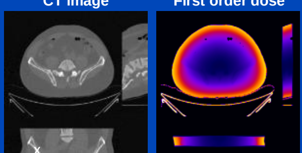


| | MC | DDE |
|---|---|---|
| 48 slices | 1 h | 0.25 s |
| whole body | 20 h | 5 s |

MC uses 16 CPU kernels
DDE uses one Nvidia Quadro P600 GPU

DDE training took 74 h for 300 epochs, 1440 samples, 48 slices per sample

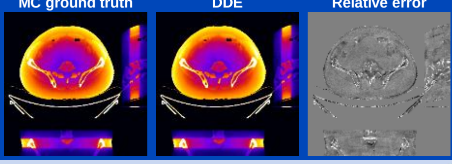


*C* = 0%
*W* = 40%

J. Maier, E. Eulig, S. Sawall, and M. Kachelrieß. Real-time patient-specific CT dose estimation using a deep convolutional neural network, Proc. IEEE MIC 2018 and ECR Book of Abstracts 2019. *Best Paper within Machine Learning at ECR 2019!*

dkfz.

# Results

## Pelvis, tube B, 120 kV, no bowtie

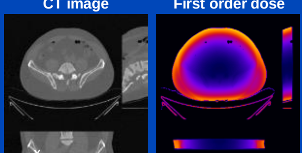


| | MC | DDE |
|---|---|---|
| 48 slices | 1 h | 0.25 s |
| whole body | 20 h | 5 s |

MC uses 16 CPU kernels
DDE uses one Nvidia Quadro P600 GPU

DDE training took 74 h for 300 epochs, 1440 samples, 48 slices per sample

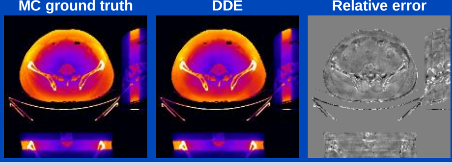


*C* = 0%
*W* = 40%

J. Maier, E. Eulig, S. Sawall, and M. Kachelrieß. Real-time patient-specific CT dose estimation using a deep convolutional neural network, Proc. IEEE MIC 2018 and ECR Book of Abstracts 2019. *Best Paper within Machine Learning at ECR 2019!*

dkfz.

## Conclusions on DDE

- As shown, DDE works well with 360° circle scans.
- What is not shown in this presentation is that DDE can be trained to provide accurate dose predictions
  - for sequence scans
  - for partial scans (less than 360°)
  - for spiral scans
  - for different tube voltages
  - for scans with and without bowtie filtration
  - for scans with tube current modulation
- In practice it may therefore be not necessary to perform separate training runs for these cases.
- Thus, accurate real-time patient dose estimation may become feasible with DDE.

J. Maier, E. Eulig, S. Sawall, and M. Kachelrieß. Real-time patient-specific CT dose estimation using a deep convolutional neural network, Proc. IEEE MIC 2018 and ECR Book of Abstracts 2019. *Best Paper within Machine Learning at ECR 2019!*

dkfz.

## Part 4:

## Image Reconstruction

dkfz.

## Often "Just" Image Restoration

- Speeding up iterative reconstruction by training a CNN to convert an FBP image into an iterative image
  - Canon's AiCE algorithm
  - GE's True Fidelity algorithm
  - plus a few more algorithms proposed in the literature
- Noise reduction by training, e.g. a mapping from low dose to high dose images
  - many examples in the literature, some in this presentation
- Artifact reduction in image domain
  - many examples in the literature, one shown in this presentation
- …

dkfz.

## Sometimes "Real" Image Reconstruction

- Networks employing data consistency layers
- Networks including backprojection layers
- Learning of backprojectors
- End-to-end training from sinogram to image
- Unrolled iterative reconstruction with learned priors
- …

dkfz.

## Sparse CT Recon with Data Consistency Layers (DCLs)

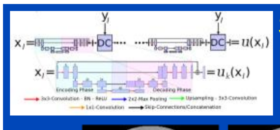

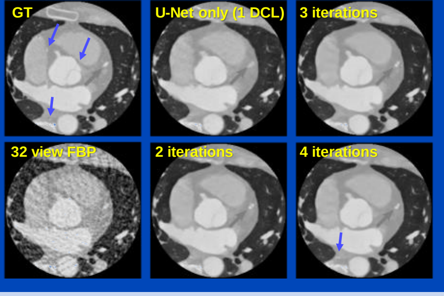


A. Kofler, M. Haltmeier, C. Kolbitsch, M. Kachelrieß, and M. Dewey. A U-Nets Cascade for Sparse View Computed Tomography, MICCAI 2018

dkfz.

## Variational Network-Based Image Reconstruction

$$C(\boldsymbol{f}) = \|\boldsymbol{X}\cdot\boldsymbol{f}-\boldsymbol{p}\|_{\boldsymbol{W}}^2 + R(\boldsymbol{f})$$
$$\nabla C(\boldsymbol{f}) = \boldsymbol{X}^{\mathrm{T}}\cdot\boldsymbol{W}\cdot(\boldsymbol{X}\cdot\boldsymbol{f}-\boldsymbol{p}) + \nabla R(\boldsymbol{f})$$
$$\boldsymbol{f}^{(t+1)} = \boldsymbol{f}^{(t)} - \lambda\nabla C(\boldsymbol{f}^{(t)})$$

Highly simplified example. Varnets work for a much wider class of cost functions whose NN-based minimization is motivated by the primal dual approach.

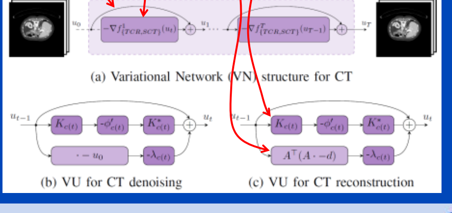


E. Kobler, R. Otazo et al. Variational network learning for low-dose CT. Proc. 5th CT-Meeting:430-434, 2018.

dkfz.

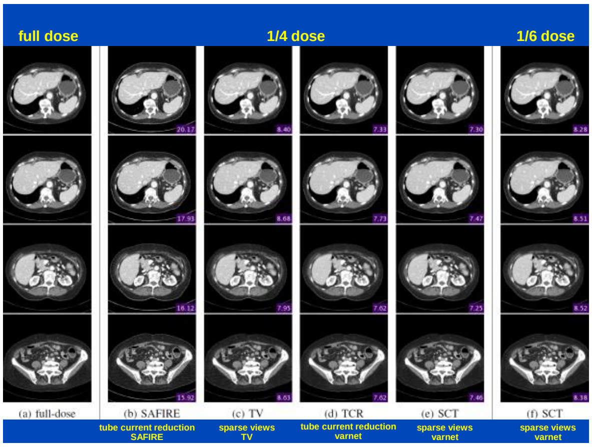


## Conclusions on Deep CT

- Machine learning will play a significant role in CT image formation.
- High potential for
  - Artifact correction
  - Noise and dose reduction
  - Real-time dose assessment (also for RT)
  - …
- Care has to be taken
  - Underdetermined acquisition, e.g. sparse view or limited angle CT, require the net to make up information!
  - Nice looking images do not necessarily represent the ground truth.
  - Data consistency layers and variational networks with rawdata access may ensure that the information that is made up is consistent with the measured data.
  - …

## Thank You!


This presentation will soon be available at www.dkfz.de/ct.
Job opportunities through DKFZ's international Fellowship programs (marc.kachelriess@dkfz.de).
Parts of the reconstruction software were provided by RayConStruct® GmbH, Nürnberg, Germany.